



The 19th International Symposium on Transportation and Traffic Theory

## A generalized integrated corridor diversion control model for freeway incident management

Yue Liu<sup>a,1\*</sup>, Gang-Len Chang<sup>b</sup>

<sup>a</sup>*Department of Civil Engineering and Mechanics, University of Wisconsin - Milwaukee, P.O. Box 784, Milwaukee, WI 53201-0784, USA.*

<sup>b</sup>*Department of Civil and Environmental Engineering, University of Maryland, College Park, MD 20742, USA.*

---

### Abstract

This paper presents a generalized diversion control model for freeway incident management that is capable of concurrently optimizing the detour rates and arterial signal timings over multiple roadway corridor segments between the freeway and its neighboring arterial. To capture various operational complexities due to the interactions between multiple diversions, this study has extended the model developed in our previous work (Liu et al., 2009), and integrated it in the overall corridor optimization process. The proposed generalized model based on reliable sensor data can produce the following three types of control parameters: 1) a set of critical upstream off-ramps and downstream on-ramps to be used for detour operations; 2) dynamic diversion rates and detour destinations for traffic at those critical upstream off-ramps within the control boundaries; and 3) arterial signal timings during the control time period. Numerical tests with a hypothetical corridor network have demonstrated the potential of the developed model for use on incident management.

© 2010 Published by Elsevier Ltd.

*Keywords:* Freeway operation; traffic flow; integrated control; diversion; incident management

---

### 1. Introduction

Traffic delays on urban freeways due to congestion have significantly undermined the efficiency and mobility of the highway systems in the United States. Most of those delays are due to non-recurrent traffic congestion caused by the reduced capacity and overwhelming demand on critical metropolitan corridors coupled with long incident durations. In such conditions, if proper diversion control strategies could be implemented in time, motorists can circumvent the congested segments by detouring through parallel arterials. To properly guide such operations, the responsible agency needs to implement effective strategies in a timely manner at all critical control points within the corridor system, including off-ramps and arterial intersections.

To contend with this vital operational issue, transportation professionals have proposed a variety of traffic diversion control and route guidance strategies, which may prioritize either system-optimal or user-optimal traffic conditions within the freeway corridor system. Responsive route guidance strategies (Messmer et al., 1994; Mammara et al., 1996) have been first proposed to provide guiding plans for traffic, based on current measurements from the

---

\* Corresponding author. Tel.: +1-414-229-3857; fax: +1-414-229-6958.

E-mail address: [yueliu1980@gmail.com](mailto:yueliu1980@gmail.com).

surveillance system, without using mathematical models in real time. Most of those strategies are localized in nature, i.e., they only generate independent plans for each off-ramp or diversion point. Extending such simple responsive strategies, multivariable responsive strategies, as well as heuristics and advanced feedback control concepts, have been developed to address the low sensitivity issue with respect to varying demands and driver compliance rates (Hawas and Mahmassani, 1995; Pavlis and Papageorgiou, 1999; Wang and Papageorgiou, 2000). Responsive route guidance strategies, though have been shown to considerably reduce travel delays compared with the no-control case, are unlikely to achieve the system-optimal traffic state due to the local nature of their control. Also, these strategies cannot provide information about future traffic conditions under current route guidance settings, which may limit their applications in a large traffic corridor network.

As an extension to responsive strategies, predictive strategies (Morin, 1995; Messmer et al., 1998; Wang et al., 2002) have been proposed, which employ a dynamic network flow model to predict future traffic conditions under the current route guidance settings, based on the current traffic state, control inputs, and predicted future demands. Compared with responsive strategies alone, these methods are generally more robust and are preferable when the corridor network has long links. However, more research and field experience are needed to verify their applicability under different topological and traffic conditions, especially under non-recurrent traffic congestion.

Another category of diversion control is called the iterative strategy, which runs a freeway network model in real time with a route guidance plan adjusting at each time interval to ensure the successful achievement of the control goal. Therefore, they are predictive in nature and may aim at achieving either the system-optimal or user-optimal condition. For the system-optimal case, a set of control formulations usually aims at minimizing a specific network performance index under the constraints of splitting rates at diversion points over a preset time horizon (Papageorgiou, 1990; Lafortune et al., 1993; Iftar, 1995; Messmer and Papageorgiou, 1995; Wie et al., 1995). On the other hand, several studies have also focused on establishing user-optimal conditions via iterative route guidance strategies (Mahmassani and Peeta, 1993; Ben-Akiva et al., 1997; Wisten and Smith, 1997; Wang et al., 2001). A key procedure embedded in those strategies is to modify the path assignment or splitting rates appropriately to reduce travel time differences among all alternative routes, which are evaluated by iteratively running a simulation model over a given time horizon.

In the past two decades, researchers began to realize the benefits of integrating freeway traffic diversion with other control measures to maximize the corridor operational performance. Several studies have documented the benefits of ramp metering with diversion over the scenario with no metering controls. Nsour et al. (1992) investigated the impacts of freeway ramp metering, with and without diversion, on traffic flow. Their results suggested that, with proper ramp metering control and coordinated arterial signal timings, the level of service for the entire corridor could be improved. However, their study ignored the interaction of traffic flow between freeway and surface streets. Similar investigation can also be found in (Moreno-Banos et al., 1993; Elloumi et al., 1996). More advanced integrated diversion strategies have also been developed to generate optimal route guidance schemes combined with other control measures (Ben-Akiva et al., 2001; Kotsialos et al., 2002), to provide routing with reliability (Kaparias et al., 2007; Nie and Wu, 2010), and to consider real-world driver behavior patterns (Paz and Peeta, 2009).

In view of the impact of detour flows on arterial traffic, a handful of integrated control models for mixed freeway and urban corridor have been formulated to produce diversion strategies and arterial signal timing adjustment jointly rather than independently. Most of the research focuses on developing non-linear optimization models for determination of various corridor control strategies either simultaneously or sequentially. Cremer and Schoof (1989) first formulated an integrated control model, in which a two-level optimization framework was proposed with the upper-level for diversion optimization and the lower-level for optimization of ramp metering, speed limit, and intersection signal timings. In their model, the control variables are not optimized concurrently and the coordination of signals on surface streets is not considered. Zhang and Hobeika (1997) proposed a nonlinear programming model to determine diversion routes and rates, ramp metering rates, and arterial signal timings for a freeway corridor under incident conditions. Their optimization model was capable of preventing congestion by limiting queue lengths with constraints and penalizing long queues in the objective function. However, delays at on-ramps and off-ramps were neglected in their model, and only stop delays on the freeway and arterial intersections were considered. Chang et al. (1993) presented a dynamic control model for a commuting corridor, including a freeway and parallel arterial. With the assumption that traffic diversion and route choice of all traffic demands were predictable, their approach features

incorporating ramp metering and intersection signal timing variables into a single optimization model and solving it simultaneously in a system-optimal fashion.

To improve the computing efficiency, other methods have been proposed in the literature by either linearizing the network flow formulations or employing the rolling solution techniques. Papageorgiou (1995) developed a linear optimal-control model to design integrated control strategies for traffic corridors, including both motorways and signal-controlled urban roads based on the store-and-forward modeling philosophy. Wu and Chang (1999) formulated a linear programming system for integrated corridor control in which the flow-density relation was approximated with a piece-wise linear function to facilitate the use of a successive linear programming algorithm for global optimality. Van den Berg et al. (2001) proposed a model predictive control approach for mixed urban and freeway networks, based on the enhanced macroscopic traffic flow models in which traffic flow evolution on ramps has been explicitly captured.

Despite the promising progress from those integrated diversion control models, only limited studies have been done regarding the multi-route diversion control, which can best demonstrate its effectiveness under the following two scenarios: 1) Under a severe lane-blockage incident. When a severe lane-blockage incident occurs on a freeway mainline segment, its impact may quickly exceed the boundaries of a single-segment corridor and spill back to its upstream ramps; and 2) With insufficient ramp and turning lane capacity. The effectiveness of detour operations is usually constrained by the available capacity at ramps and intersection turning lanes. Implementation of detour operations only for the incident segment may not be effective if the demand surge due to diversion results in a bottleneck at the ramps.

In response to the above research needs, this paper develops a model for integrated diversion control of a multi-segment corridor, in which multiple detour routes comprising several on-ramps, off-ramps, and several segments of parallel arterials are employed to coordinately divert traffic under incident conditions. The proposed model is designed to have the following operational features: 1) Selecting a set of critical upstream off-ramps and downstream on-ramps for use in the detour operations within each control interval (i.e. the control boundaries) so as to assist traffic operators in better prioritizing the limited control resources; 2) Capturing various operational complexities due to the interactions between multiple diversion decisions as well as their impacts on arterial traffic patterns in a dynamic control environment; 3) Determining the dynamic diversion rates and detour destinations for traffic at upstream off-ramps to effectively utilize the available capacity in the parallel arterials; and 4) Updating arterial signal timings to prevent the formation of local bottlenecks due to detour traffic.

This paper is organized as follows. Next section will present an extended corridor network flow model that can capture the interactions among multiple detouring traffic and their impacts on the local arterial. Grounded on the above formulation, Section 3 illustrates the optimal diversion control model with the objectives of maximizing the utilization of corridor capacity and concurrently minimizing the total time of detour traffic. The model was solved with a genetic-algorithm-based heuristic, and extensive numerical analyses with a 12-mile hypothetical corridor network are summarized in Section 4. Concluding comments along with key findings are reported in the last section.

## **2. The extended corridor model**

In our previous work by, an integrated corridor model has been developed to capture the traffic dynamics in the arterial, freeway section, and on-off ramps. However, the application of the model is limited to the control area including only one segment of the freeway mainline experiencing the incident, an off-ramp upstream to the incident location, a parallel arterial, and an on-ramp right after the incident location. This section aims to extend the base model to cover multiple segments of a corridor network. The extended model is expected to capture explicitly the evolution of multi-route detour traffic along the ramps and surface streets as well as the resulting local bottlenecks caused by the dramatic change in traffic demand levels and patterns due to diversion operations. Those unique modeling features, when properly integrated with the traditional freeway model, can more accurately and effectively set the control variables in the overall corridor optimization process. To ensure the integrality of the model presentation, this section has also included the key formulations developed in Liu et al. (2009) when necessary:

2.1. Arterial dynamics

In modeling the arterial traffic dynamics, this study has employed a lane-group-based model to capture the interactions between multiple detouring traffic as well as their impacts on local arterial. The lane-group-based model has shown its effectiveness in modeling severe congestion situation in the arterials (Liu et al., 2008), and has been employed to design efficient signal timings (Liu and Chang, 2010). The key concept is to decompose the evolution process of traffic flow on a given arterial link into six subsets, including demand origins, upstream arrivals, propagating to the end of queue, merging into lane groups, departure, and flow conservation (see Fig. 1). In this section, the lane-group-based model is extended to incorporate the impacts of multiple detouring traffic flows heading to different downstream on-ramps. Key variables and parameters used in the model presentation are given in Table 1:

Table 1 List of key variables used in the extended model for arterial dynamics

|   |   |
|---|---|
| $\Delta t$  | Update interval of arterial dynamics (in seconds)   |
| $k$   | Time step index corresponds to time $t = k\Delta t$   |
| $n, n \in S_N$  | Index of arterial intersections   |
| $i, i \in S^U$  | Index of links  |
| $S^{OUT}$   | Set of outgoing boundary links in the arterial  |
| $S_{\mu}^+, S_{\mu}^-$  | Set of on-ramps upstream and downstream of the incident location  |
| $S_V^+, S_V^-$  | Set of off-ramps upstream and downstream of the incident location   |
| $\mu, \nu$  | Index of the on-ramps and off-ramps, respectively   |
| $p, p \in P_n$  | Index of signal phase at the intersection $n$   |
| $S_r$   | Set of traffic demand entries   |
| $\Gamma(i), \Gamma^{-1}(i)$                                       | Set of upstream and downstream links of link $i$  |
| $l_i, n_i, N_i, Q_i$  | Length (in meters), # of lanes, storage capacity (in vehs), and discharge capacity (in vph) of link $i$   |
| $m, m \in S_m^M$  | Index of lane groups at link $i$  |
| $\delta_{m,j}^i, j \in \Gamma^{-1}(i)$                            | A binary indicating whether the movement from link $i$ to $j$ uses lane group $m$   |
| $N_m^i, Q_m^i$  | Storage capacity (in vehs) and discharge capacity (in vph) for lane group $m$   |
| $D_r[k], r \in S_r$   | Flow rate generated at demand entry $r$ at step $k$ (in vph)  |
| $IN_r[k], r \in S_r$  | Flow rate entering the link from demand entry $r$ at step $k$ (in vph)  |
| $w_r[k], r \in S_r$   | Queue waiting on the entry $r$ at step $k$ (in vehs)  |
| $q_i^{in}[k]$   | Num. of upstream inflow vehicles of link $i$ at step $k$ (in vehs)  |
| $\bar{n}_i[k]$  | Num. of vehicles from normal arterial traffic at link $i$ at step $k$ (in vehs)   |
| $N_{\mu}^i[k], \mu \in S_{\mu}^-$                                 | Num. of detour vehicles heading to downstream on-ramp $\mu$ at link $i$ at step $k$ (in vehs)   |
| $\bar{\gamma}_{ij}[k], j \in \Gamma^{-1}(i)$                      | Relative turning proportion of normal arterial traffic from link $i$ to $j$   |
| $\gamma_{ij}^{\mu}, j \in \Gamma^{-1}(i), \mu \in S_{\mu}^-$      | A binary value indicating whether detour traffic at link $i$ heading to downstream on-ramp $\mu$ will use downstream link $j$ or not            |
| $\eta_i[k]$   | Fraction of normal arterial traffic in total traffic at link $i$ at step $k$  |
| $\theta_{\mu}^i[k], \mu \in S_{\mu}^-$                            | Fraction of traffic heading to downstream on-ramp $\mu$ within the total detour traffic at step $k$   |
| $s_i[k]$  | Available space of link $i$ at step $k$ (in vehs)   |
| $x_i[k]$  | Num. of vehicles in queue at link $i$ at step $k$ (in vehs)   |
| $q_i^{arr}[k]$  | Num. of vehicles arriving at end of queue of link $i$ at step $k$ (in vehs)   |
| $q_m^{i,pot}[k]$  | Num. of vehicles potentially to merge into lane group $m$ of link $i$ at step $k$ (in vehs)   |
| $q_m^i[k]$  | Num. of vehicles join the queue of lane group $m$ at step $k$ (in vehs)   |
| $x_m^i[k]$  | Queue length of lane group $m$ at link $i$ at step $k$ (in vehs)  |
| $\bar{x}_m^i[k]$  | Num. of arrival vehicles with destination to lane group $m$ queued outside the approach lanes due to blockage at link $i$ at step $k$ (in vehs) |
| $\lambda_{m,j}^i[k], j \in \Gamma^{-1}(i)$                        | Percentage of movement from link $i$ to $j$ in lane group $m$   |
| $\bar{\lambda}_{m,j}^i[k], j \in \Gamma^{-1}(i)$                  | Percentage of normal arterial traffic in lane group $m$ going from link $i$ to $j$  |
| $\lambda_{m,j}^{\mu}[k], j \in \Gamma^{-1}(i), \mu \in S_{\mu}^-$ | Percentage of detour traffic in lane group $m$ going from link $i$ to $j$ with destination to on-ramp $\mu$ .                                   |
| $Q_m^i[k]$  | Num. of vehicles depart from lane group $m$ at link $i$ at step $k$ (in vehs)   |
| $Q_{ij}^{pot}[k]$   | Num. of vehicles potentially depart from link $i$ to link $j$ at step $k$ (in vehs)   |
| $Q_{ij}^i[k]$   | Total flows actually depart from link $i$ to link $j$ at step $k$ (in vehs)   |
| $\bar{Q}_{ij}^i[k]$   | Normal arterial traffic flows actually depart from link $i$ to link $j$ at step $k$ (in vehs)   |
| $Q_{ij}^{\mu}[k], \mu \in S_{\mu}^-$                              | Detour traffic flows heading to downstream on-ramp $\mu$ actually depart from link $i$ to link $j$ at step $k$ (in vehs)                        |

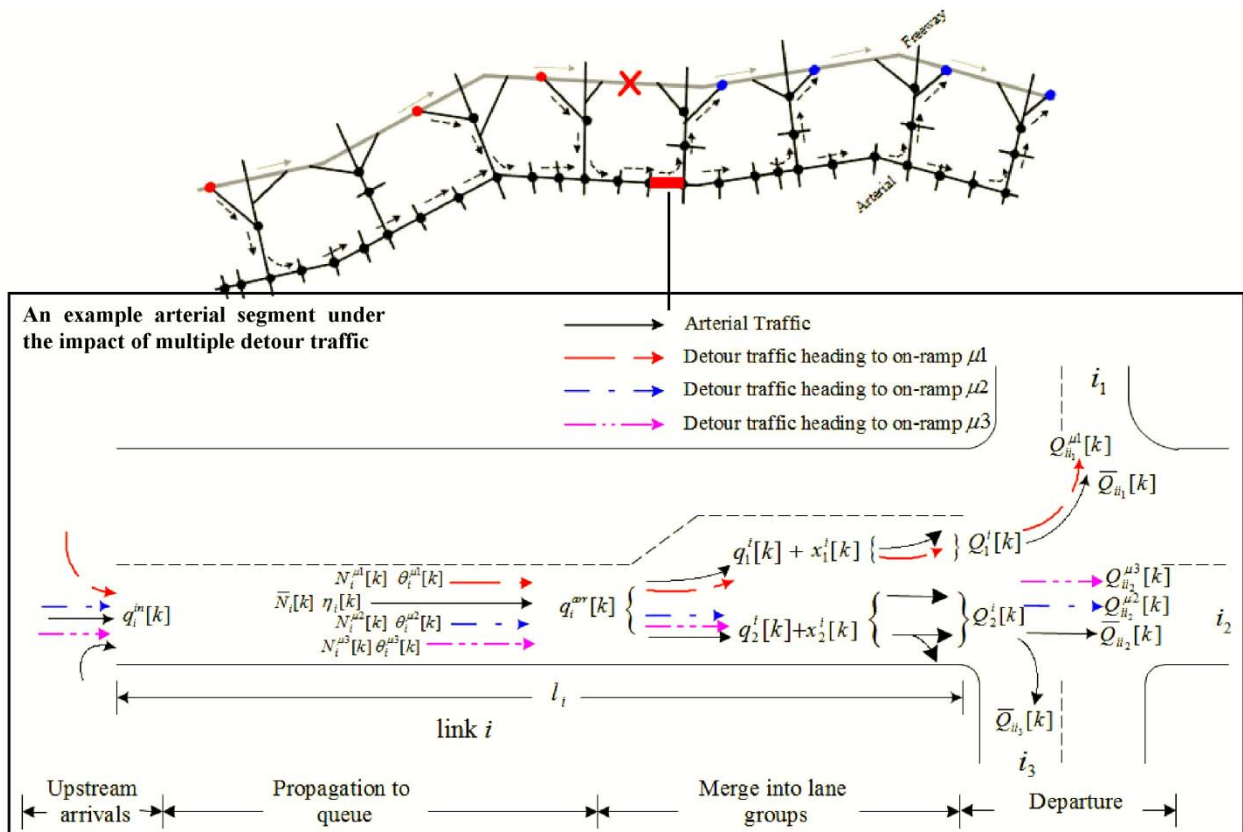


Fig. 1 Illustration of the interactions between multiple detouring traffic and their impacts on local arterial

2.1.1. Demand Origins

Arterial demand entries are modeled as follows:

$$IN_r[k] = \min \left[ D_r[k] + \frac{w_r[k]}{\Delta t}, Q_r, \frac{s_i[k]}{\Delta t} \right] \tag{1}$$

$$w_r[k+1] = w_r[k] + \Delta t [D_r[k] - IN_r[k]] \tag{2}$$

Equation 1) indicates that the flow rate enters the arterial link  $i$  from demand entry  $r$  depends on the existing flows queuing at  $r$ , discharge capacity of the link  $i$ , and the available space in link  $i$ . Equation 2) updates the queue level at the demand entry at each time step  $k$ .

2.1.2. Upstream Arrivals

Considering the presence of multiple detouring traffic, the upstream arrival process for an internal arterial link  $i$  can be formulated with Equation 3):

$$q_i^{in}[k] = \sum_{j \in \Gamma(i)} \bar{Q}_{ji}[k] + \sum_{\mu \in S_i} \sum_{j \in \Gamma(i)} Q_{ji}^{\mu}[k] \tag{3}$$

Where,  $\bar{Q}_{ji}[k]$  and  $Q_{ji}^{\mu}[k]$  represent the actual flows departing from upstream link  $j$  to link  $i$  for arterial traffic and detour traffic heading to on-ramp  $\mu$ , respectively. Therefore, the upstream arrival flows at link  $i$  is modeled as the sum of actual departure flows from all upstream links, including both arterial and multiple detouring traffic.

For source links (connected with demand entry  $r$ ), inflows can be formulated as:

$$q_i^{in}[k] = IN_r[k] \cdot \Delta t \tag{4}$$

2.1.3. Propagation to the End of Queue

This set of dynamic equations represents the evolution of upstream inflows to the end of queue with the average approaching speed. The mean speed of vehicles,  $v_i[k]$ , depending on the density of the segment between the link upstream and the end of queue,  $\rho_i[k]$ , can be described with the following equation (Ben-Akiva, 1996):

$$v_i[k] = \begin{cases} v_i^{free}, & \text{if } \rho_i[k] < \rho^{min} \\ v^{min} + (v_i^{free} - v^{min}) \cdot \left[ 1 - \left( \frac{\rho_i[k] - \rho^{min}}{\rho^{jam} - \rho^{min}} \right)^\alpha \right]^\beta, & \rho_i[k] \in [\rho^{min}, \rho^{jam}] \\ v^{min}, & \text{if } \rho_i[k] > \rho^{jam} \end{cases} \quad (5)$$

where,  $v_i[k]$  represents the mean approaching speed of vehicles from upstream to the end of queue at link  $i$  at step  $k$ ;  $\rho^{min}$  is the minimum critical density below which traffic at link  $i$  moves at free flow speed  $v_i^{free}$ ;  $v^{min}$  is the minimum traffic flow speed corresponding the jam density  $\rho^{jam}$ .  $\alpha, \beta$  are constant model parameters to be calibrated.  $\rho_i[k]$  can be computed with the following equation:

$$\rho_i[k] = \frac{\bar{N}_i[k] + \sum_{\mu \in S_\mu^-} N_i^\mu[k] - x_i[k]}{n_i \left( l_i - \frac{1000 \cdot x_i[k]}{n_i \cdot \rho^{jam}} \right)} \quad (6)$$

where,  $\bar{N}_i[k] + \sum_{\mu \in S_\mu^-} N_i^\mu[k] - x_i[k]$  represents the number of vehicles (both arterial and detour traffic) moving at the segment between the link upstream and the end of queue, and  $l_i - 1000 \cdot x_i[k] / (n_i \cdot \rho^{jam})$  approximates the length of that segment over time. Then, the number of vehicles arriving at the end of queue at link  $i$  (see Fig. 1) can be dynamically updated with:

$$q_i^{arr}[k] = \min \{ \rho_i[k] \cdot v_i[k] \cdot n_i \cdot \Delta t, \bar{N}_i[k] + \sum_{\mu \in S_\mu^-} N_i^\mu[k] - x_i[k] \} \quad (7)$$

where,  $\rho_i[k] \cdot v_i[k] \cdot n_i \cdot \Delta t$  represents the flows potentially arriving at the end of queue at time step  $k$ , which is limited by  $\bar{N}_i[k] + \sum_{\mu \in S_\mu^-} N_i^\mu[k] - x_i[k]$ .

2.1.4. Merging into Lane Groups

As shown in Fig. 1, after vehicles arrive at the end of queue at a link, they will try to change lanes and merge into different lane groups, based on their local and detour destinations. The number of vehicles that can actually merge into their destination lane group  $m$  at time step  $k$  is determined with Equation 8):

$$q_m^i[k] = \min \left\{ \max \{ N_m^i - x_m^i[k], 0 \}, \max \left\{ q_m^{i,pot}[k] \cdot \left[ 1 - \sum_{m' \in S_i^M} \omega_{m'm}^i[k] \right], 0 \right\} \right\} \quad (8)$$

and  $q_m^{i,pot}[k]$  is given by:

$$q_m^{i,pot}[k] = \tilde{x}_m^i[k] + \sum_{j \in \Gamma^{-1}(i)} q_i^{arr}[k] \cdot \left[ \eta_i[k] \cdot \tilde{\gamma}_{ij}^i[k] + \sum_{\mu \in S_\mu^-} (1 - \eta_i[k]) \cdot \theta_i^\mu[k] \cdot \gamma_{ij}^\mu \right] \cdot \delta_m^{ij} \quad (9)$$

In Equation 8),  $\max \{ N_m^i - x_m^i[k], 0 \}$  denotes the available storage capacity in lane group  $m$  at time step  $k$ , and  $\max \left\{ q_m^{i,pot}[k] \cdot \left[ 1 - \sum_{m' \in S_i^M} \omega_{m'm}^i[k] \right], 0 \right\}$  is the maximum allowable flows to merge into lane group  $m$  considering the potential queue blockage effects from other lane groups (e.g. a fully occupied through lane group may completely block the left-turn traffic). Thus,  $q_m^i[k]$  should be the minimum of those two values.

In our previous work, a blocking matrix concept has been introduced to model the queue interactions among lane groups. A detailed description on the blocking matrix can be found in Liu et al. (2008), where  $\omega_{m',m}^i[k]$  is one element of the blocking matrix to model the discount of the merging capacity for lane group  $m$  due to the blockage from lane group  $m'$ . Considering blockages from all possible lane groups, one can use  $1 - \sum_{m \in S_i^M \wedge m' \neq m} \omega_{m',m}^i[k]$  to represent

the residual fraction of capacity to accommodate the potential level of flows that may merge into lane group  $m$  at time step  $k$ , given by Equation 9). Note that in Equation 9),  $q_i^{arr}[k]$  is the total flows arriving at the end of queue of link  $i$  at time step  $k$ ;  $q_i^{arr}[k] \cdot \eta_i[k] \cdot \bar{\gamma}_{ij}$  represents the normal arterial traffic flow going to link  $j$  at time step  $k$ , and  $q_i^{arr}[k] \cdot \sum_{\mu \in S_{\mu}^-} (1 - \eta_i[k]) \cdot \theta_i^{\mu}[k] \cdot \gamma_{ij}^{\mu}$  denotes the detour traffic flow going to link  $j$  at time step  $k$ ;  $\delta_m^{ij}$  is a binary

value indicating whether traffic going from link  $i$  to  $j$  uses lane group  $m$ . Hence, the total arriving flows to lane group  $m$  can be approximated with  $\sum_{j \in \Gamma^{-1}(i)} q_i^{arr}[k] \cdot \left[ \eta_i[k] \cdot \bar{\gamma}_{ij}[k] + \sum_{\mu \in S_{\mu}^-} (1 - \eta_i[k]) \cdot \theta_i^{\mu}[k] \cdot \gamma_{ij}^{\mu} \right] \cdot \delta_m^{ij}$ , which is added with  $\tilde{x}_m^i[k]$  to  $q_m^{i,pot}[k]$ .

### 2.1.5. Departing Process

The number of vehicles potentially departing from link  $i$  to link  $j$  at time step  $k$  is given by:

$$Q_{ij}^{pot}[k] = \sum_{m \in S_i^M} \min \{ q_m^i[k] + x_m^i[k], Q_m^i \cdot g_n^p[k] \} \cdot \lambda_m^{ij}[k] \tag{10}$$

and  $\lambda_m^{ij}[k]$  is given by:

$$\lambda_m^{ij}[k] = \frac{\delta_m^{ij} \cdot \left[ \eta_i[k] \bar{\gamma}_{ij}[k] + \sum_{\mu \in S_{\mu}^-} (1 - \eta_i[k]) \theta_i^{\mu}[k] \gamma_{ij}^{\mu} \right]}{\sum_{j \in \Gamma^{-1}(i)} \delta_m^{ij} \cdot \left[ \eta_i[k] \bar{\gamma}_{ij}[k] + \sum_{\mu \in S_{\mu}^-} (1 - \eta_i[k]) \theta_i^{\mu}[k] \gamma_{ij}^{\mu} \right]} \tag{11}$$

where,  $\min \{ q_m^i[k] + x_m^i[k], Q_m^i \cdot g_n^p[k] \}$  depicts the flows potentially departing from lane group  $m$  at time step  $k$ ;  $g_n^p[k]$  is a binary value indicating whether signal phase  $p$  of intersection  $n$  is set to green at step  $k$ ;  $\lambda_m^{ij}[k]$  is the percentage of traffic in lane group  $m$  going from link  $i$  to  $j$ . Therefore,  $\min \{ q_m^i[k] + x_m^i[k], Q_m^i \cdot g_n^p[k] \} \cdot \lambda_m^{ij}[k]$  reflects the flows potentially departing from link  $i$  to  $j$  in lane group  $m$ , and the summation of it over all lane groups in link  $i$  comes to Equation 10). Assuming that a total of one unit flow is to depart from link  $i$  at time step  $k$ ,  $\eta_i[k] \bar{\gamma}_{ij}[k] + \sum_{\mu \in S_{\mu}^-} (1 - \eta_i[k]) \theta_i^{\mu}[k] \gamma_{ij}^{\mu}$  will be the amount of flows within that one unit to go to link  $j$ , and

$\delta_m^{ij} \cdot \left[ \eta_i[k] \bar{\gamma}_{ij}[k] + \sum_{\mu \in S_{\mu}^-} (1 - \eta_i[k]) \theta_i^{\mu}[k] \gamma_{ij}^{\mu} \right]$  will be the amount of flows going to link  $j$  by lane group  $m$ , and

$\sum_{j \in \Gamma^{-1}(i)} \delta_m^{ij} \cdot \left[ \eta_i[k] \bar{\gamma}_{ij}[k] + \sum_{\mu \in S_{\mu}^-} (1 - \eta_i[k]) \theta_i^{\mu}[k] \gamma_{ij}^{\mu} \right]$  will be the total amount of flows departing from lane group  $m$ .

Hence,  $\lambda_m^{ij}[k]$  can be approximated with Equation 11). Similarly, the percentage of arterial traffic in lane group  $m$  going from link  $i$  to  $j$ ,  $\bar{\lambda}_m^{ij}[k]$ , can be approximated by Equation 12):

$$\bar{\lambda}_m^{ij}[k] = \frac{\delta_m^{ij} \cdot \eta_i[k] \bar{\gamma}_{ij}[k]}{\sum_{j \in \Gamma^{-1}(i)} \delta_m^{ij} \cdot \left[ \eta_i[k] \bar{\gamma}_{ij}[k] + \sum_{\mu \in S_\mu^-} (1 - \eta_i[k]) \theta_i^\mu[k] \gamma_{ij}^\mu \right]} \quad (12)$$

and, the percentage of detour traffic in lane group  $m$  going from link  $i$  to  $j$  heading to on-ramp  $\mu$  can be obtained with:

$$\lambda_m^{ij\mu}[k] = \frac{\delta_m^{ij} \cdot (1 - \eta_i[k]) \theta_i^\mu[k] \gamma_{ij}^\mu}{\sum_{j \in \Gamma^{-1}(i)} \delta_m^{ij} \cdot \left[ \eta_i[k] \bar{\gamma}_{ij}[k] + \sum_{\mu \in S_\mu^-} (1 - \eta_i[k]) \theta_i^\mu[k] \gamma_{ij}^\mu \right]} \quad (13)$$

In addition, due to the limitation of storage capacity in the downstream links, the actual number of vehicles departing from link  $i$  to link  $j$  at time step  $k$  is given by:

$$Q_{ij}[k] = \max \left\{ 0, \min \left\{ Q_{ij}^{pot}[k], \frac{Q_{ij}^{pot}[k]}{\sum_{i \in \Gamma(j)} Q_{ij}^{pot}[k]} \cdot s_j[k] \right\} \right\} \quad (14)$$

where,  $s_j[k]$  is the available space in link  $j$  at time step  $k$ , and  $Q_{ij}^{pot}[k] / \sum_{i \in \Gamma(j)} Q_{ij}^{pot}[k]$  is the proportion of the available space in link  $j$  allocated to accommodate flows from link  $i$ .

After obtaining the values of  $Q_{ij}[k]$ ,  $\lambda_m^{ij}[k]$ ,  $\bar{\lambda}_m^{ij}[k]$ , and  $\lambda_m^{ij\mu}[k]$ , one can estimate the actual departing flows from lane group  $m$  at time step  $k$  as:

$$Q_m^i[k] = \sum_{j \in \Gamma^{-1}(i)} Q_{ij}[k] \cdot \delta_m^{ij} \quad (15)$$

Finally, the actual departing flow of arterial traffic from link  $i$  to link  $j$  at time step  $k$  is given by:

$$\bar{Q}_{ij}[k] = \sum_{m \in S_i^M} Q_m^i[k] \cdot \bar{\lambda}_m^{ij}[k] \quad (16)$$

and the actual departing flow of detour traffic from link  $i$  to link  $j$  heading to on-ramp  $\mu$  at time step  $k$  is given by:

$$Q_{ij}^\mu[k] = \sum_{m \in S_i^M} Q_m^i[k] \cdot \lambda_m^{ij\mu}[k], \mu \in S_\mu^- \quad (17)$$

Note that, we have  $\bar{Q}_{ij}[k] + \sum_{\mu \in S_\mu^-} Q_{ij}^\mu[k] = Q_{ij}[k]$  holds.

### 2.1.6. Flow Conservation

Based on the estimation of the arrivals and departures in an arterial link, key traffic state variables can be updated following the flow conservation law. The lane group based queues are advanced as follows:

$$x_m^i[k+1] = x_m^i[k] + q_m^i[k] - Q_m^i[k] \quad (18)$$

Queues outside the approach lanes due to overflows or blockages are advanced as follows:

$$\tilde{x}_m^i[k+1] = \tilde{x}_m^i[k] - q_m^i[k] + \sum_{j \in \Gamma^{-1}(i)} q_i^{arr}[k] \cdot \left[ \eta_i[k] \cdot \bar{\gamma}_{ij}[k] + \sum_{\mu \in S_\mu^-} (1 - \eta_i[k]) \cdot \theta_i^\mu[k] \cdot \gamma_{ij}^\mu \right] \cdot \delta_m^{ij} \quad (19)$$

Based on Equations 18) and 19), the total vehicle queue at link  $i$  is computed as:

$$x_i[k+1] = \sum_{m \in S_i^M} (x_m^i[k+1] + \tilde{x}_m^i[k+1]) \quad (20)$$

The evolution of the total number of normal arterial vehicles at link  $i$  can be stated as:

$$\bar{N}_i[k+1] = \bar{N}_i[k] + \sum_{j \in \Gamma(i)} \bar{Q}_{ji}[k] - \sum_{j \in \Gamma^{-1}(i)} \bar{Q}_{ij}[k] \quad (21)$$

The evolution of the detour traffic at link  $i$  heading to on-ramp  $\mu$  can be stated as:

$$N_i^\mu[k+1] = N_i^\mu[k] + \sum_{j \in \Gamma(i)} Q_{ji}^\mu[k] - \sum_{j \in \Gamma^{-1}(i)} Q_{ij}^\mu[k], \mu \in S_\mu^- \quad (22)$$

Based on Equations 21) and 22), the fraction of normal arterial traffic at link  $i$  is updated as:

$$\eta_i[k+1] = \frac{\bar{N}_i[k+1]}{\bar{N}_i[k+1] + \sum_{\mu \in S_\mu^-} N_i^\mu[k+1]} \quad (23)$$

and the fraction of traffic heading to downstream on-ramp  $\mu$  within the total detour traffic can be updated as:

$$\theta_i^\mu[k+1] = \frac{N_i^\mu[k+1]}{\sum_{\mu \in S_\mu^-} N_i^\mu[k+1]}, \mu \in S_\mu^- \quad (24)$$

Finally, one can compute the available storage space of link  $i$  as follows:

$$s_i[k+1] = N_i - \bar{N}_i[k+1] - \sum_{\mu \in S_\mu^-} N_i^\mu[k+1] \quad (24)$$

## 2.2. Freeway and Ramps

The macroscopic traffic flow model proposed by Messer and Papageorgiou was employed in this study to model the traffic evolution for the freeway section. The key concept is to divide the freeway link into homogeneous segments, and update the flow, density, and speed within each segment at every time interval ( $\Delta T$ ). Detailed model formulation can be found in Messer and Papageorgiou (1990) and will not be presented in this paper.

As on-ramps and off-ramps function to exchange diversion flows between the freeway and arterial system, this study has employed the lane-group-based concept to model on-ramps and off-ramps so that the freeway and arterial traffic dynamics can be connected into an overall corridor model.

### 2.2.1. On-ramp

As illustrated in Fig. 2, the on-ramp can be modeled as a simplified arterial link with only one lane group and one downstream link. The only difference between an on-ramp and an arterial link is the departing process. Since the update step for freeway ( $\Delta T$ ) is larger than the one for arterial ( $\Delta t$ ), this study has employed the approach by Van den Berg (2001) to keep consistency between the indices of time steps for the two systems ( $t$  is the time index for freeway and  $k$  is for arterial, and  $k = l \cdot t$ ,  $l = \Delta T / \Delta t$ ). Therefore, the actual flow that departs from on-ramp  $\mu$  into freeway at time step  $k$  between  $l \cdot t$  and  $l \cdot (t+1) - 1$  is given by:

$$Q_\mu[k] = \frac{Q_\mu[t] \cdot \Delta T}{l}, \quad \forall k \in [l \cdot t, l \cdot (t+1) - 1] \quad (25)$$

and  $Q_\mu[t]$  is computed by:

$$Q_\mu[t] = \min \left( \frac{x_\mu[l \cdot t] + \sum_{k=lt}^{l(t+1)-1} q_\mu^{arr}[k]}{\Delta T}, Q_\mu \cdot \min \left[ 1, \frac{\rho^{jam} - \rho_{i+1,0}[t]}{\rho^{jam} - \rho_i^{crit}} \right] \right) \quad (26)$$

where,  $x_\mu[l \cdot t] + \sum_{k=lt}^{l(t+1)-1} q_\mu^{arr}[k]$  is the potential number of vehicles to merge into freeway mainline from on-ramp  $\mu$

at the freeway update time step  $t$ ;  $Q_\mu$  is the discharge capacity of on-ramp  $\mu$ ;  $\rho^{jam}$  is jam density for freeway,  $\rho_{i+1,0}[t]$  is the density of freeway segment immediate downstream of the on-ramp  $\mu$ , and  $\rho_i^{crit}$  is the critical density of freeway link  $i$ .

2.2.2. Off-ramp

Similarly, the off-ramp could also be modeled as an arterial link if the upstream arrival process is modified properly, as shown in Fig. 2. The actual flow that enters off-ramp  $\nu$  at each arterial time step  $k$  between  $l \cdot t$  and  $l \cdot (t+1) - 1$  is given by:

$$q_{\nu}^{in}[k] = \frac{q_{\nu}^{in}[t] \cdot \Delta T}{l}, \quad \forall k \in [l \cdot t, l \cdot (t+1) - 1] \tag{27}$$

and  $q_{\nu}^{in}[t]$  is given by:

$$q_{\nu}^{in}[t] = \min\left\{ \rho_{i-1, N(i-1)}[t] \cdot v_{i-1, N(i-1)}[t] \cdot n_{i-1, N(i-1)} \cdot (\gamma_{\nu}^h + \delta_{\nu\mu}^h \cdot \beta_{\nu}^h \cdot Z_{\nu}^h), \right. \\ \left. Q_{\nu}, \frac{s_{\nu}[l \cdot t] + \sum_{k=lt}^{l(t+1)-1} \sum_{j \in \Gamma^{-1}(\nu)} Q_{\nu j}[k]}{\Delta T} \right\} \tag{28}$$

where,  $\rho_{i-1, N(i-1)}[t]$ ,  $v_{i-1, N(i-1)}[t]$ , and  $n_{i-1, N(i-1)}$  represent the density, speed, and number of lanes at the segment immediate upstream to the off-ramp  $\nu$ , respectively.  $\gamma_{\nu}^h$  is the normal exit rate for off-ramp  $\nu$  during control time interval  $h$ ;  $Z_{\nu}^h$  is the diversion control rate to be optimized during the control interval  $h$ ;  $\beta_{\nu}^h$  is the driver compliance rate to the detour operation during control interval  $h$ ;  $\delta_{\nu\mu}^h$  is a binary decision variable indicating whether traffic at off-ramp  $\nu$  will be diverted to downstream on-ramp  $\mu$  during the control interval  $h$  (1 – Yes, 0 –

No);  $Q_{\nu}$  represents the capacity of off-ramp  $\nu$ , and  $s_{\nu}[l \cdot t] + \sum_{k=lt}^{l(t+1)-1} \sum_{j \in \Gamma^{-1}(\nu)} Q_{\nu j}[k]$  is the available space at off-ramp  $\nu$ .

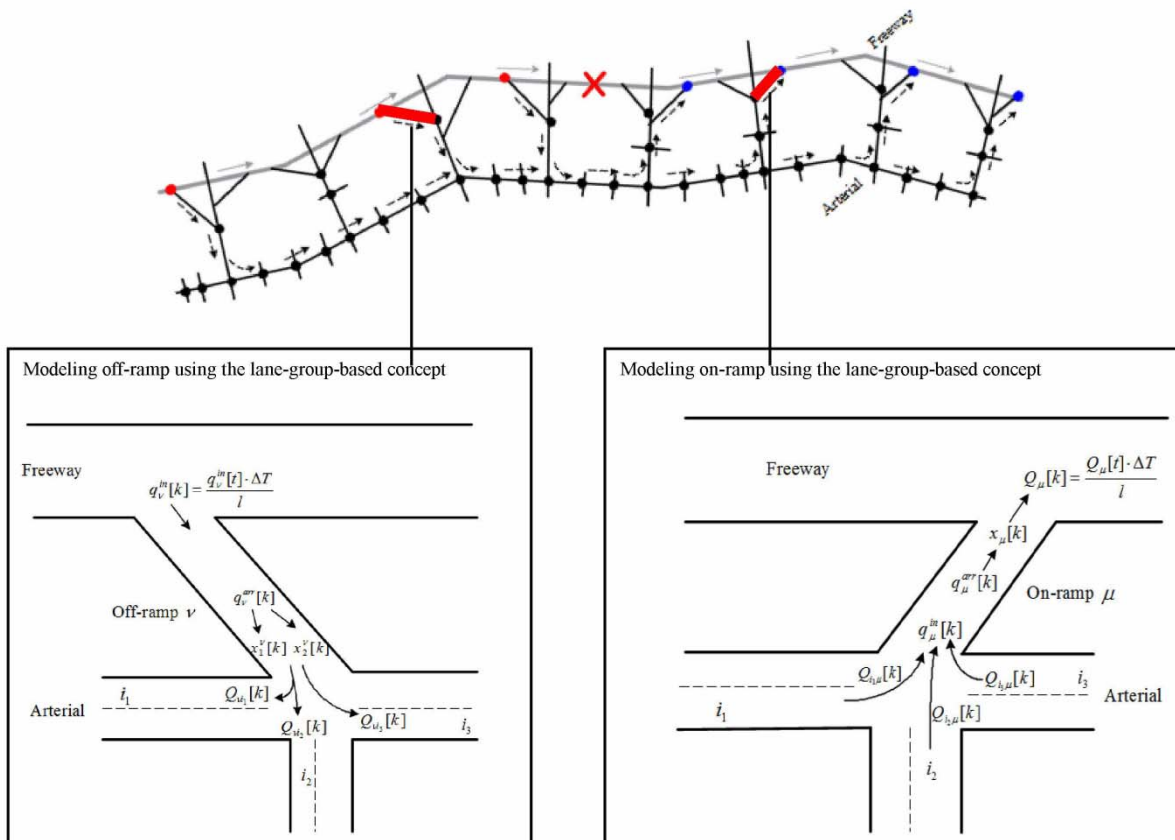


Fig. 2 Traffic flow dynamics at on-ramps and off-ramps

### 3. The control model and solution

With the above extended overall corridor flow model, one can then construct a diversion control model that can yield the following outputs, including 1) a set of critical upstream off-ramps and downstream on-ramps to be used for detour operations (i.e. the control boundaries); 2) dynamic diversion rates and detour destinations for traffic at those critical upstream off-ramps within the incident impact boundaries; and 3) arterial signal timings including cycle lengths, offsets, and green splits.

#### 3.1. Objective Functions

Given the entire control time period  $H$ , the model aims to maximize the utilization of available arterial capacity, and increase the total corridor throughput, given by:

$$f_1 : - \left[ \sum_{t=1}^H q_{i+1,0}[t] \cdot \Delta T + \sum_{k=1}^H \sum_{i \in S^{OUT}} q_i^{in}[k] \right] \tag{29}$$

where,  $q_{i+1,0}[t]$  represents the total number of vehicles entering the downstream freeway link in the corridor network, and  $\sum_{k=1}^H \sum_{i \in S^{OUT}} q_i^{in}[k]$  denotes the total number of vehicles entering the boundary links in the arterial.

Another objective function of the control model is designed to reflect the perspective of detour travelers, which aims at minimizing their total time spent on the detour route so as to ensure their compliance to the routing guidance. This objective is given by:

$$f_2 : \sum_{k=1}^H \left[ \sum_{i \in S^U} \sum_{\mu \in S_{\mu}^-} N_i^{\mu}[k] + \sum_{v \in S_v^+} \sum_{\mu \in S_{\mu}^-} N_v^{\mu}[k] + \sum_{\mu \in S_{\mu}^-} N_{\mu}^{\mu}[k] \right] \cdot \Delta t \tag{30}$$

Where,  $N_i^{\mu}[k]$ ,  $N_v^{\mu}[k]$ , and  $N_{\mu}^{\mu}[k]$  represent the number of detour vehicles heading to on-ramp  $\mu$  that are traveling at link  $i$ , off-ramp  $v$ , and on-ramp  $\mu$  within the incident impact boundaries at time step  $k$ , respectively.

#### 3.2. Decision Variables

The decision variables include the following five sets:

- $\{C^h, h \in H\}$  Common cycle length for all intersections in the control interval  $h$  ;
- $\{\Delta_n^h, \forall n \in S_N, h \in H\}$  Offset of intersection  $n$  for each control interval  $h$  ;
- $\{G_{np}^h, \forall n \in S_N, p \in P_n, h \in H\}$  Green time for phase  $p$  of intersection  $n$  for each control interval  $h$  ;
- $\{\delta_{v\mu}^h, v \in S_v^+, \mu \in S_{\mu}^-, h \in H\}$  Dynamic detour plans from upstream off-ramp  $v$  to downstream on-ramp  $\mu$  within the incident impact boundaries;
- $\{Z_v^h, v \in S_v^+, h \in H\}$  Diversion rates at the incident upstream off-ramp  $v$  for each control interval  $h$  ;

#### 3.3. Constraints

The extended corridor model formulations presented in Section 2 constitute the principal constraints for the control model. In addition, this study has employed the following operational constraints for the control decision variables:

$$C^{\min} \leq C^h \leq C^{\max} \tag{31}$$

$$G_{np}^{\min} \leq G_{np}^h < C^h, \forall n \in S_N, p \in P_n, h \in H \tag{32}$$

$$\sum_{p \in P_n} G_{np}^h + \sum_{p \in P_n} I_{np} = C^h, \forall n \in S_N, p \in P_n, h \in H \tag{33}$$

$$0 \leq \Delta_n^h < C^h, \forall n \in S_N, h \in H \tag{34}$$

$$\beta_v^h \cdot Z_v^h + \gamma_v^h \leq Z^{\max}, \forall v \in S_v^+, h \in H \tag{35}$$

where,  $C^{\min}$  and  $C^{\max}$  are the minimum and maximum cycle length, respectively;  $P_n$  is the set of signal phases at intersection  $n$ ;  $G_{np}^{\min}$  is the minimal green time for phase  $p$  of intersection  $n$ ; and  $I_{np}$  represents the inter-green time for phase  $p$  of intersection  $n$ .  $Z^{\max}$  is the maximum percentage of traffic (including both detour and normal exiting) that can diverge from freeway to arterial. Equation 31) restricts the common cycle length to be between the minimal and maximal values. Equation 32) requires that the green time for each phase should at least satisfy the minimal green time and no more than the cycle length. And, the sum of green times and inter-greens for all phases at intersection  $n$  should be equal to the cycle length by Equation 33). Moreover, the offset of intersection  $n$  is constrained by Equation 34) to be between 0 and the cycle length. The diversion rate is bounded by Equation 35).

In addition to the above operational constraints, this study has also defined that traffic at any upstream off-ramp can be detoured to no more than one downstream on-ramp during the same control interval  $h$ , given by:

$$\sum_{\mu \in S_{\mu}^-} \delta_{v\mu}^h \leq 1, \quad \forall v \in S_v^+, h \in H \tag{36}$$

In summary, the mathematical expression of the proposed generalized corridor control model is given below:

$$\begin{aligned} \min \quad & \Phi(s) = \begin{bmatrix} f_1(s) \\ f_2(s) \end{bmatrix} \\ f_1 : & - \left[ \sum_{t=1}^H q_{i+1,0}[t] \cdot \Delta T + \sum_{k=1}^H \sum_{i \in S^{OUT}} q_i^{in}[k] \right] \\ f_2 : & \sum_{k=1}^H \left[ \sum_{i \in S^U} \sum_{\mu \in S_{\mu}^-} N_i^{\mu}[k] + \sum_{v \in S_v^+} \sum_{\mu \in S_{\mu}^-} N_v^{\mu}[k] + \sum_{\mu \in S_{\mu}^-} N_{\mu}^{\mu}[k] \right] \cdot \Delta t \\ s.t. \quad & s : \{C^h, \Delta_n^h, G_{np}^h, Z_v^h, \delta_{v\mu}^h, \forall h \in H\} \end{aligned} \tag{37}$$

### 3.4. Model Solution

This study has employed the genetic algorithm integrated with the rolling time horizon approach to solve the proposed model. The two objectives in the control model are first normalized into the same scales, and then weighted to a single function for optimization, given by:

$$r(s) = \sqrt{w_1 \cdot \left( \frac{f_1(s) - f_1^{\min}(P)}{f_1^{\max}(P) - f_1^{\min}(P)} \right)^2 + w_2 \cdot \left( \frac{f_2(s) - f_2^{\min}(P)}{f_2^{\max}(P) - f_2^{\min}(P)} \right)^2}, s \in P \tag{38}$$

where,  $s \in P$  represents the solution  $s$  in the current population  $P$ ;  $w_m$  ( $m=1,2$ ) is the weight assigned to objective function  $m$  to emphasize its degree of importance.  $f_m^{\min}(P) = \min\{f_m(s) | s \in P\}$  and  $f_m^{\max}(P) = \max\{f_m(s) | s \in P\}$  represent the minimum and the maximum values of the objective function at the current population  $P$ , respectively. Note that, the smaller the  $r(s)$  is, the better the individual will be in the current GA population. Details about the GA searching procedure and decoding schemes are not the focus of this paper and can be found in Liu et al. (2009).

The rolling time horizon approach optimizes the control plans over successive stages, based on the projection of traffic conditions within each stage. The optimized control plan is only implemented within the first control interval of that stage. Then, the optimization process starts all over again with feedback from the real-time surveillance system, and the control horizon shifts forward by one control interval. In real-world applications, lengths of the projection stage and the control update interval need to be carefully set in order to perform a trade-off between the computing efficiency and the model accuracy.

## 4. Case study

### 4.1. Experimental Design

To illustrate the applicability of the generalized corridor model, this study has employed a hypothetical corridor which includes 12 freeway exits and 36 arterial intersections for numerical tests. Basic layouts of the corridor network are given in Fig. 3.

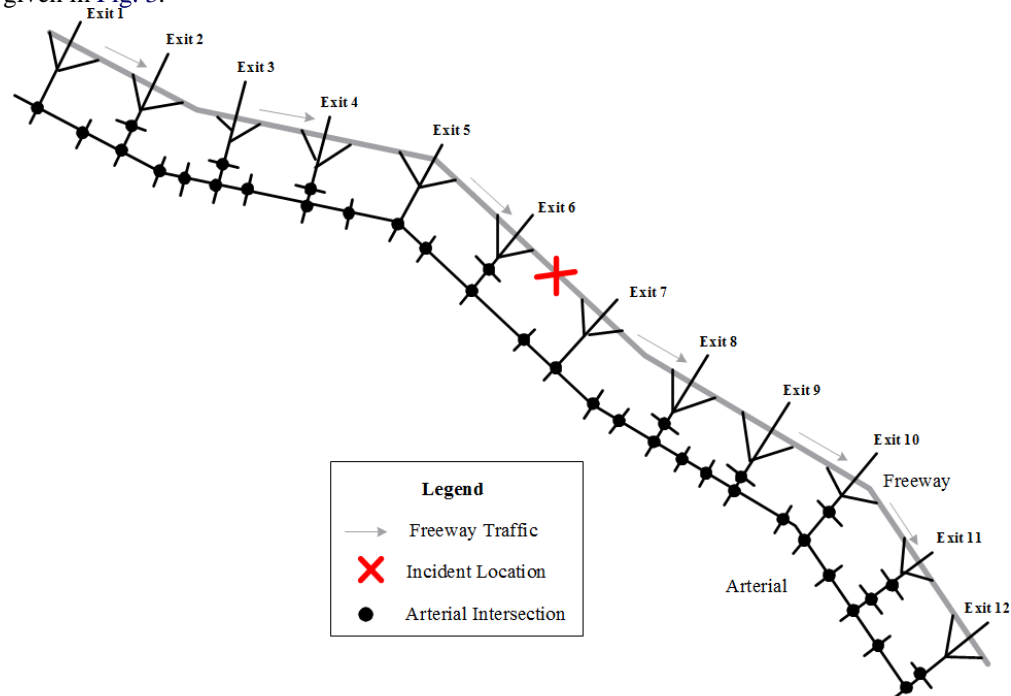


Fig. 3 A hypothetical corridor network for case study

Assuming that an incident occurs on the freeway mainline section (between Exit 6 and 7), the proposed control model will determine a set of critical off-ramps and on-ramps for detour operations, and update the control measures, including diversion rates at critical upstream off-ramps and signal timings at all related intersections. The entire experiment period is designed to be 60 minutes, including the first interval of 5-min for normal operations (no incident), the second interval of 40-min with incident, and the final interval of 15-min for recovery. The key data used for model inputs is summarized as follows:

#### Traffic Demand Related

- Freeway entry volumes: 3000 vph;
- Normal arterial entry volumes: 500 vph for arterial (80% for through and right-turn, 20% for left-turn); 200 vph for the side streets (40% for left-turn, 40% for right-turn, and 20% for through);
- Normal exiting rate at the off-ramps is 5% for the entire control time horizon;
- Driver compliance rates to the detour operation at all off-ramps are assumed at the 100% level over entire control time period;

#### Traffic Model Related

- Update time steps for the arterial ( $\Delta t$ ) and the freeway ( $\Delta T$ ) are set to be 1s and 5s, respectively;
- Each freeway segment is set to be 800ft;
- Jam density  $\rho^{jam}$  is set to be 210veh/mile/lane, and the minimum density  $\rho^{min}$  is set to be 20veh/mile/lane;
- Discharge capacity: freeway (2200vplph), arterial link (1800vplph), ramps (1900vplph);
- Average vehicle length is set to be 24 ft to compute the storage capacity of arterial links;
- Arterial traffic flow model parameters:  $\alpha$  (3.0),  $\beta$  (2.0);

- All other traffic flow parameters used in the extended corridor model take the same values as in Liu et al. (2009);
- 40% freeway capacity is available after the incident;

Geometry Related

- The number of lanes on the affected freeway mainline: 2;
- The number full lanes at the arterial: 2;
- The number of left-turn lanes at arterial: 1;
- The number of lanes at off-ramps and on-ramps: 1;

Control Related

- Maximum diversion rate (0.5);
- Minimum and maximum cycle length for arterial intersections: (60s), (160s);
- Each arterial intersection has four phases with the left-turn lag in the arterial direction and split phase for the side streets;
- Minimum green time per phase: (7s), clearance time (5s);

Optimization Algorithm Related

- The GA population size is set at 100;
- The maximum number of generation is set at 200;
- The crossover probability is set at 0.6;
- The mutation probability is set at 0.02;
- The length of the projection stage for the rolling time window approach is set to be 10-min, and the control update interval is set to be twice of the arterial cycle length;

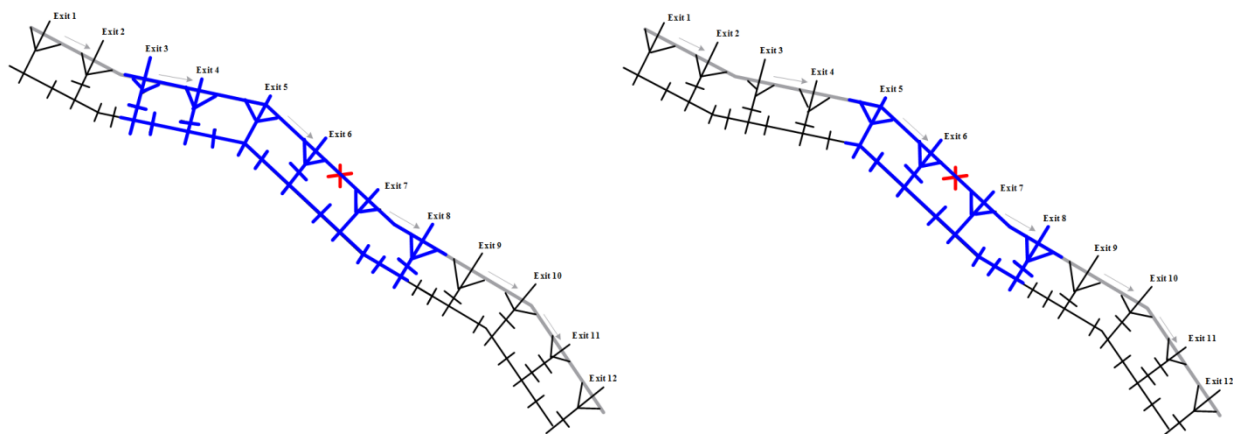
4.2. Experimental Analysis and Results

Since the base version of the integrated diversion control model has shown significant improvement on operational efficiency as validated through an example of a single corridor segment in our previous work, this section will evaluate the extended model with emphasis on the following aspects:

- The impacts of different weight assignment settings on the control area (critical off-ramps and on-ramps involved) generated from the proposed model and the system MOEs; and
- Comparison of the extended model performance with the base model under the same incident scenario and the same control objective.

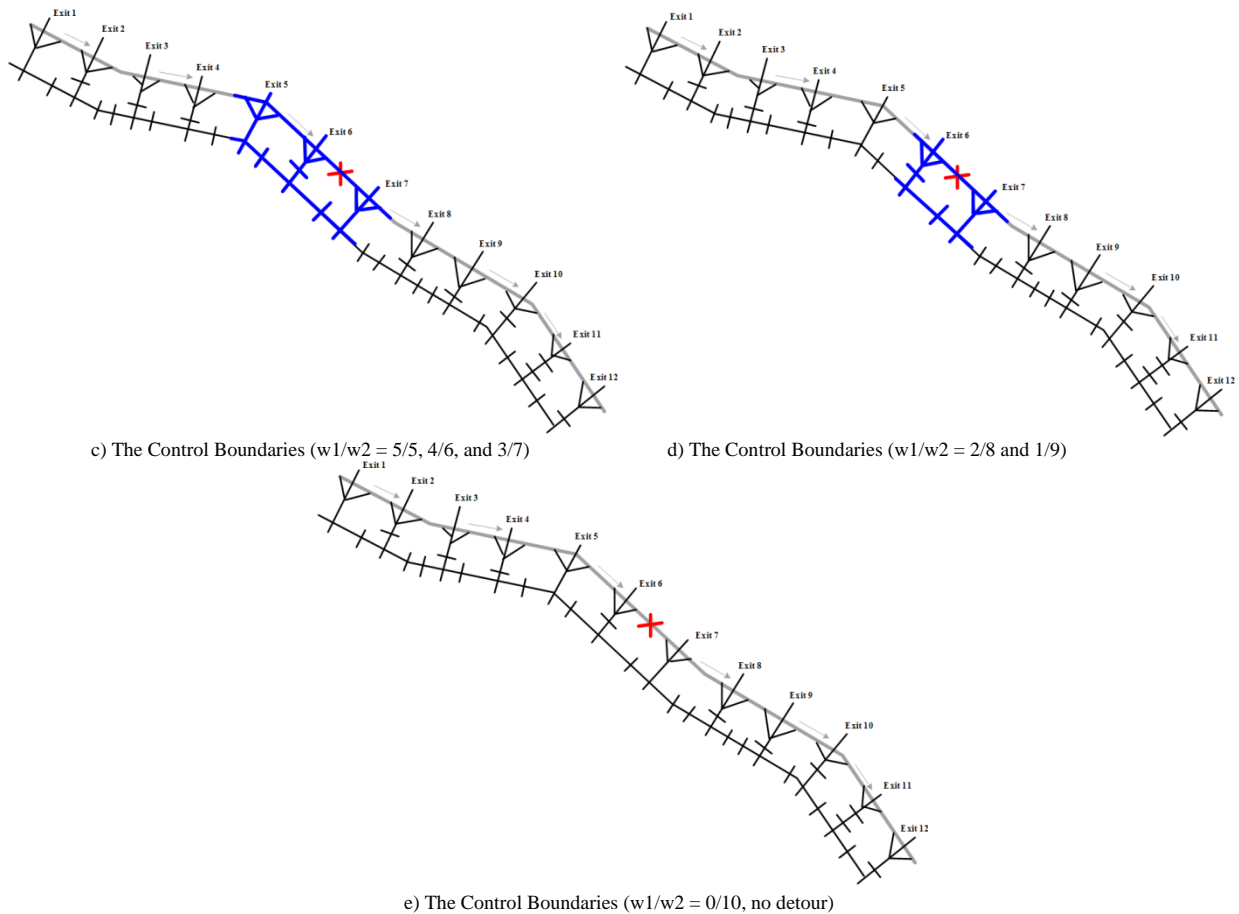
4.2.1. The impact of different assigned weights on the control boundaries and system MOEs

Fig. 4 presents the variation of the generated control boundaries (shown in the blue color) with the assigned weights of  $w_1 / w_2$  ranging from 10/0 to 0/10 for the study corridor network.



a) The Control Boundaries ( $w_1/w_2 = 10/0$  and  $9/1$ )

b) The Control Boundaries ( $w_1/w_2 = 8/2, 7/3$  and  $6/4$ )



**Fig. 4** The control boundaries generated from the model under different weight assignment

The variation of the control boundaries and its impact on the system MOEs are summarized in Table 2. Comparison between the results yields the following observations:

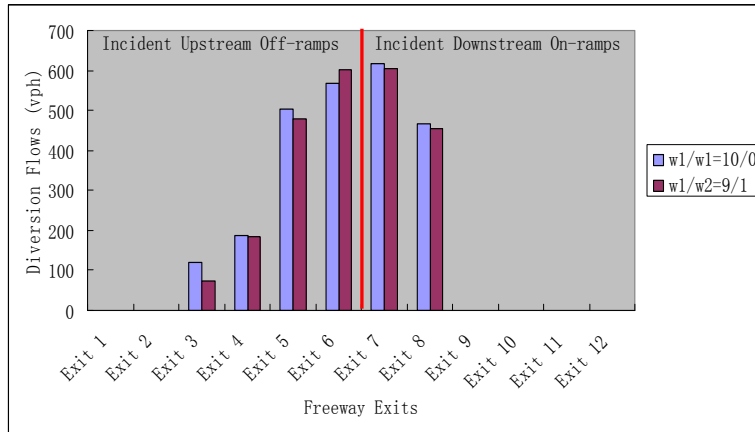
- With the weight assignment between two control objectives varying from 10/0 to 0/10, the generated control area shrinks and the total diversion rate decreases as expected;
- Depending on the traffic conditions and corridor network structure, there exists a critical control area beyond which the total corridor throughput no longer increases. For example, although the study network covers a 12-exit stretch, only 4 upstream exits and 2 downstream exits are used to yield the maximal corridor throughput (see Fig. 4-a);
- The number of incident downstream on-ramps used to divert traffic back to the freeway is less than that of incident upstream off-ramps, which is expected since the higher capacity at incident-free freeway links may encourage detour traffic to come back to the freeway whenever it is available; and
- Compared with the control boundaries generated by maximizing the total corridor throughput only (i.e.,  $w_1/w_2 = 10/0$ ), the one obtained by setting  $w_1/w_2 = 8/2$  seems more appropriate for the example corridor network due to its compact size and shorter distances for detour operations (Fig. 4-a v.s. Fig. 4-b), which can significantly save the manpower and control resources. Most importantly, it can substantially reduce the required total diversion rates as well as the total time spent by the detour traffic (12.3% and 19.8%, respectively, as highlighted in Table 2) at the relatively low reduction in the total corridor throughput (3.2% as shown in Table 2). In real-world applications, traffic operators can refer to the same procedure to determine the proper control boundaries, and achieve the maximal control benefits under the given incident scenario.

**Table 2** System MOEs under various weight assignment

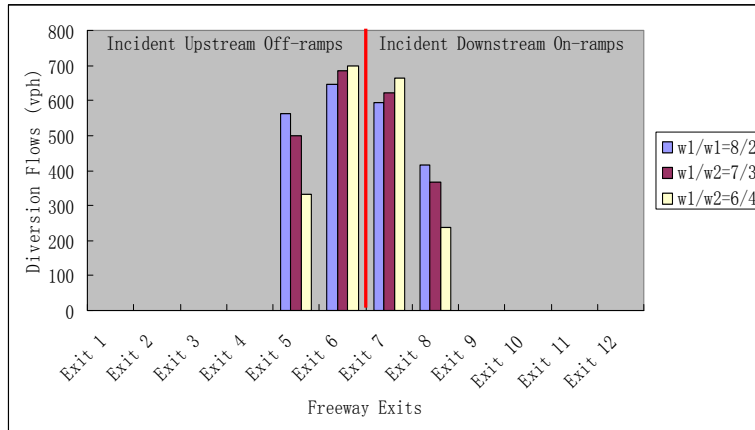
| $w_1 / w_2$ | Corridor System MOE              |                             |  |
|-------------|----------------------------------|-----------------------------|--|
|             | Total Corridor Throughput (vehs) | Total Diversion Rates (vph) | Total Time Spent by Detour Traffic (veh-min) |
| 10/0        | 3352                             | 1379                        | 4573.8                                       |
| 9/1         | 3297                             | 1340                        | 4441.5                                       |
| 8/2         | 3244 (-3.2%)                     | 1209 (-12.3%)               | 3667.4 (-19.8%)                              |
| 7/3         | 3198                             | 1176                        | 3330.5                                       |
| 6/4         | 3077                             | 1030                        | 2937.8                                       |
| 5/5         | 2835                             | 799                         | 2231   |
| 4/6         | 2764                             | 701                         | 1842.7                                       |
| 3/7         | 2694                             | 596                         | 1544.1                                       |
| 2/8         | 2570                             | 404                         | 987.5  |
| 1/9         | 2476                             | 288                         | 694.3  |
| 0/10        | 2226                             | 0                           | 0.0  |

This experimental analysis has also yielded the distribution of diversion flows over different off-ramps and on-ramps within the control area under various weights between two control objectives. The comparison results, as shown in Fig. 5, have indicated that:

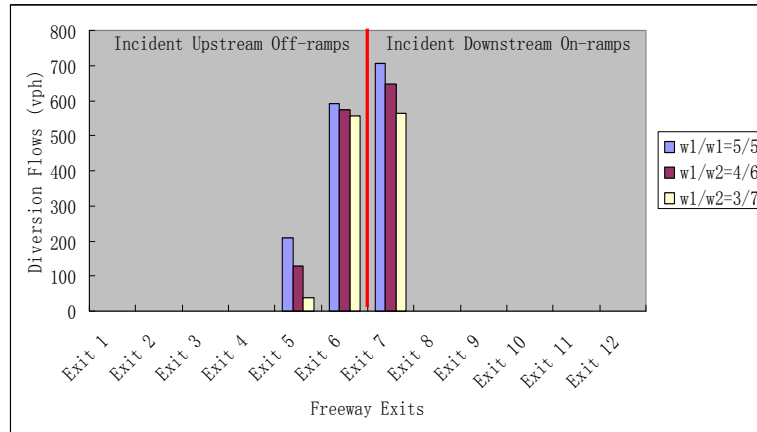
- The diversion flows are not evenly distributed over the ramps. An off-ramp closer to the incident location has carried most diversion flows, and the on-ramp closer to the incident location has also received more detoured flows (see Fig. 5). This is reasonable as traffic prefers to reduce the extra travel distances caused by the detour operations, and comes back to the freeway as soon as possible to best use the high capacity at incident-downstream freeway links; and
- Traffic operators shall set weights to obtain a proper control area without those marginal ramps (e.g. exit 3 and 4 in Fig. 5-a), as they incur some excessive detour times, but not substantially contribute to the increase of total corridor throughput;



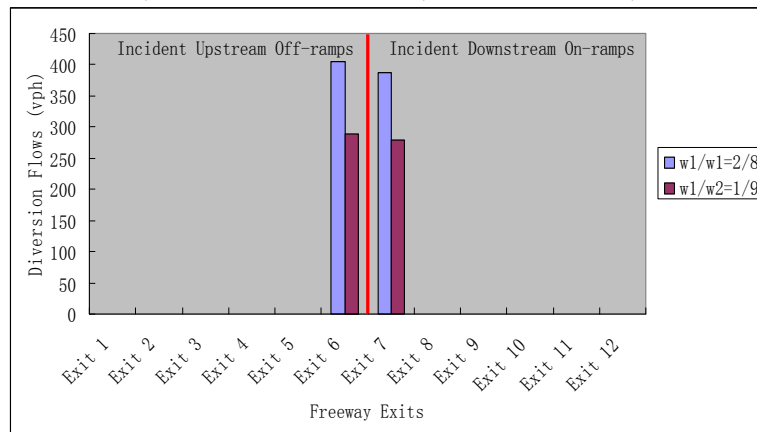
a) Distribution of Diversion Flows ( $w_1/w_2 = 10/0$  and  $9/1$ )



b) Distribution of Diversion Flows ( $w_1/w_2 = 8/2$ ,  $7/3$  and  $6/4$ )



c) Distribution of Diversion Flows (w1/w2 = 5/5, 4/6, and 3/7)



d) Distribution of Diversion Flows (w1/w2 = 2/8 and 1/9)

Fig. 5 Distribution of diversion flows under different weight assignment

#### 4.2.2. Comparison between the extended model and base model

In this analysis, the performance of the extended model will be compared with its base version to validate the effectiveness of multi-route diversion control for incident management. The study network shown in Fig. 3 with the same experimental design is employed for comparison. The performance of the following two control models is compared with CORSIM:

- Model 1 - The base model proposed in our previous work (Liu et al., 2009) with only one segment between exits 6 and 7 as the control area, and the control objective is to maximize the total corridor throughput; and
- Model 2 - The extended model proposed in this study with the control objective of maximizing the total corridor throughput.

Fig. 6 illustrates the difference in control areas for the above two models, and Table 3 summarizes the comparison results between the two models with respect to the following four types of performance indices:

- Total diversion rate
- Total corridor throughput
- Average detour link total queue time
- Average side street link total queue time

Comparison between the results in Table 3 yields the following observations:

- The extended model outperforms the base model in terms of the total corridor throughput (i.e., 3352 versus 2917, a +14.9% increase) due to the fact that using only one corridor segment is subject to the

limitation of flow capacity at the ramp or the intersection turning lane. However, with multiple ramps for integrated diversion control, one can overcome such limitation by balancing the detour traffic load over multiple ramps and intersection turning lanes, which results in a higher rate of diversion flows (1379 versus 984) and better utilized network capacity;

- The advantage of the extended model is also indicated by the significant decrease in average total queue time on detour links (547.2 veh-min versus 416.8 veh-min, a 23.8% decrease) and at the side-street links (833.7 veh-min versus 575.9 veh-min, a 30.9% decrease). Compared with the base model, this result is desirable as it encourages traffic to follow the detour operations, and avoids the excessive delays to the side street traffic.

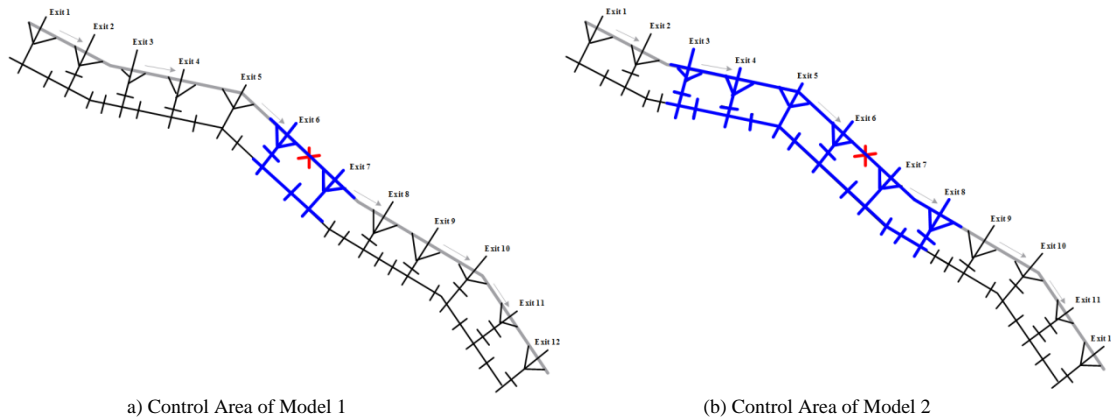


**Fig. 6** Difference in control areas for Model 1 and 2

**Table 3** Comparison results between the base model (Model 1) and the extended model (Model 2)

| Performance Indices                            | Model 1 | Model 2 | Improvement over Model 1 |
|--|---------|---------|--------------------------|
| Total diversion rates (vph)                    | 984     | 1379    | +40.1%                   |
| Total corridor throughput (vehs)               | 2917    | 3352    | +14.9%                   |
| Average detour link total queue time (veh-min) | 547.2   | 416.8   | -23.8%                   |
| Average side street total queue time (veh-min) | 833.7   | 575.9   | -30.9%                   |

### 5. Conclusion

This study has presented a generalized diversion control model for freeway incident management that is capable of concurrently optimizing the detour rates and arterial signal timings over multiple roadway segments between the freeway and its neighboring arterial. To capture various operational complexities due to the interactions between multiple diversions, this study has extended the model developed in our previous work, and integrated it in the overall corridor optimization process. Preliminary numerical tests with a hypothetical corridor network have confirmed the conclusions that:

- The generalized corridor model offers the flexibility for traffic operators to determine the proper time and control points to implement diversion control, which can help to prioritize the limited control resources and achieve the best operational efficiency;
- Compared with the base model, the generalized corridor model can substantially improve the utilization of corridor capacity by balancing the detour traffic load over multiple ramps and intersection turning lanes, which can effectively prevent the excessive delays on the detour route.

Future studies along this line will be focused on modeling the precise capacity reduction of the freeway due to the incident, and development of an efficient on-line feedback process to estimate the compliance pattern of drivers in response to the provided travel time information and their perceived traffic conditions. Further improving the computing efficiency of the proposed solution algorithm for use in a large-scale detour operation shall also be one of the priority on-going tasks.

## References

- Ben-Akiva, M. (1996). Development of a deployable real-time dynamic traffic assignment system, Task D Interim report: analytical developments for DTA system, MIT, Cambridge, MA.
- Ben-Akiva, M., Bierlaire, M., Bottom, J., Koutsopoulos H., & Mishalani, R. (1997). Development of a route guidance generation system for real-time application. In 8th IFAC/IFIP/IFORS Symposium of Transportation Systems, pp. 433–439.
- Ben-Akiva, M., Bottom, J., Ramming, M.S. (2001). Route guidance and information systems. *Journal of Systems and Control Engineering*, v 215, n 4, p 317-324.
- Chang, G. L., Ho, P. K., Wei, C. H. (1993). A dynamic system-optimum control model for commuting traffic corridors. *Transportation Research 1C*, 3-22.
- Cremer, M., Schoof, S. (1989). On control strategies for urban traffic corridors. In *Proceedings of IFAC Control, Computers, Communications in Transportation*, Paris.
- Eloumi, N., Haj-Salem, H., & Papageorgiou, M. (1996). Integrated control of traffic corridors-application of an LP-methodology. The 4th Meeting EURO Working Group on Transportation Systems, Landshut, Germany.
- Hawas, Y., Mahmassani, H.S. (1995). A decentralized scheme for real-time route guidance in vehicular traffic networks. In *Proceedings of 2nd World Congress on Intelligent Transport Systems*, pp. 1956–1963.
- Iftar, A. (1995). A decentralized routing controller for congested highways, In *Proceedings of 34th Conference on Decision and Control*. New Orleans, LA, USA, pp. 4089–4094.
- Kaparias, I., Bell, M., Chen, Y., Bogenberger, K. (2007). Icnavs: a tool for reliable dynamic route guidance. *IET Intelligent Transportation Systems 1(4)*, 225–253.
- Kotsialos, A., Papageorgiou, M., Mangeas, M., Haj-salem, H. (2002). Coordinated and integrated control of motorway networks via non-linear optimal control. *Transportation Research 10C*, 65-84.
- Lafortune, S., Sengupta, R., Kaufman, D. E., & Smith, R. L. (1993). Dynamic system-optimal traffic assignment using a state space model. *Transportation Research 27B*, 451–473.
- Liu, Y., Yu, J., Chang, G.L., Rahwanji, S. (2008). A lane-group based macroscopic model for signalized intersections account for shared lanes and blockages. *IEEE Conference on Intelligent Transportation Systems, Proceedings, ITSC*, pp. 639-644.
- Liu, Y., Chang, G. L., Yu, J. (2009). A Multi-Objective Model for Optimal Diversion Control of A Freeway Corridor under Incident Conditions, the 88th TRB Annual Meeting CD-ROM, Washington D.C..
- Liu, Y., Chang, G.-L. (2010). An arterial signal optimization model for intersections experiencing queue spillback and lane blockage. *Transportation Research Part C*, doi:10.1016/j.trc.2010.04.005, in press.
- Mahmassani, H. S., Peeta, S. (1993). Network performance under system optimal and user equilibrium dynamic assignments: implications for advanced traveler information systems. *Transportation Research Record 1408*, 83-93.
- Mammar, S., Messmer, A., Jensen, P., Papageorgiou, M., Haj-Salem, H. & Jensen, L. (1996). Automatic control of variable message signs in Aalborg. *Transportation Research 4C*, 131–150.
- Messmer, A., Papageorgiou, M. (1990). METANET: A macroscopic simulation program for motorway networks. *Traffic Engineering and Control*, 31, pp. 466-470.
- Messmer, A., Papageorgiou, M. (1994). Automatic control methods applied to freeway network traffic. *Automatica*, 30, 691–702.
- Messmer, A., Papageorgiou, M. (1995). Route diversion control in motorway networks via nonlinear optimization. *IEEE Transaction on Control System Technology*, 3, 144-154.
- Messmer, A., Papageorgiou, M., & Mackenzie, N. (1998). Automatic control of variable message signs in the interurban Scottish highway network. *Transportation Research C*, 6, 173–187.
- Moreno-Banos, J. C., Papageorgiou, M. & Schäffner, C. (1993). Integrated optimal flow control in traffic networks. *European Journal of Operations Research*, 71, 317–323.
- Morin, J.-M. (1995). Aid-to-decision for variable message sign control in motorway networks during incident condition. In *Proceedings of the 4th ASCE International Conference on Applications of Advanced Technologies in Transportation Engineering*, pp. 378–382.
- Nie, Y., Wu, X. (2010). Providing Reliable Route Guidance: A Case Study Using Chicago Data. In the 89th Transportation Research Board Annual Meeting, Washington DC, January.
- Nsour, S. A., Cohen, S. L., Clark, J. E., Santiago, A. J. (1992). Investigation of the impacts of ramp metering on traffic flow with and without diversion. *Transportation Research Record 1365*, 116-124.
- Papageorgiou, M. (1990). Dynamic modeling, assignment, and route guidance in traffic networks. *Transportation Research 24B*, 471-495.
- Papageorgiou, M. (1995). An integrated control approach for traffic corridors. *Transportation Research 3C*, 19-30.
- Pavlis, Y., Papageorgiou, M. (1999). Simple decentralized feedback strategies for route guidance in traffic networks. *Transportation Science 33*, 264–278.
- Paz, A., Peeta, S. (2009). Behavior-consistent real-time traffic routing under information provision. *Transportation Research Part C*, v 17, n 6, p 642-661.

- Van den Berg, De Schutter, A. Hegyi, B. & Hellendoorn, J. (2001). Model predictive control for mixed urban and freeway networks. *Transportation Research Record*, 1748, 55-65.
- Wang, Y., Papageorgiou, M. (2000). Feedback routing control strategies for freeway networks: A comparative study. In *Proceedings of the 2nd International Conference on Traffic and Transportation Studies*, pp. 642–649.
- Wang, Y., Messmer, A. & Papageorgiou, M. (2001). Freeway network simulation and dynamic traffic assignment using METANET tools. *Transportation Research Record* 1776, 178-188.
- Wang, Y., Papageorgiou, M. & Messmer, A. (2002). A predictive feedback routing control strategy for freeway network traffic. In *Proceedings of American Control Conference*, pp. 3606–3611.
- Wie, B., Tobin, R., Bernstein, D., & Friesz, T. (1995). Comparison of system optimum and user equilibrium dynamic traffic assignment with schedule delays. *Transportation Research* 3C, 389–411.
- Wisten, M. B., Smith, M. J. (1997). Distributed computation of dynamic traffic equilibria. *Transportation Research* 5C, 77–93.
- Wu, J., & Chang, G.L. (1999). Heuristic method for optimal diversion control in freeway corridors. *Transportation Research Record* 1667, 8-15.
- Zhang, Y., Hobeika, A. (1997). Diversion and signal re-timing for a corridor under incident conditions. In the 77th Annual Meeting of Transportation Research Board CD-ROM, Washington, DC.